

1 Auroral streamers and magnetic flux closure.

2 B. Hubert⁽¹⁾, K. Kauristie⁽²⁾, O. Amm⁽²⁾, S. E. Milan⁽³⁾, A. Grocott⁽³⁾, S. W. H.
3 Cowley⁽³⁾ and T. I. Pulkkinen⁽²⁾

4 1. Laboratory for Planetary and Atmospheric Physics, University of Liège, Belgium
5 2. Finnish Meteorological Institute, Space Research, Helsinki, Finland
6 3. Department of Physics & Astronomy, University of Leicester, Leicester LE1 7RH, UK

7 On 7 December 2000 at 2200 UT an auroral streamer was
8 observed to develop above Scandinavia with the IMAGE-FUV
9 global imagers. The ionospheric equivalent current deduced from
10 the MIRACLE-IMAGE Scandinavian ground-based network of
11 magnetometers is typical of a substorm-time streamer.
12 Observations of the proton aurora using the SI12 imager onboard
13 the IMAGE satellite are combined with measurements of the
14 ionospheric convection obtained by the SuperDARN radar
15 network to compute the dayside merging and nightside flux
16 closure rates. On the basis of this and other similar events, it is
17 found that auroral streamers appear during the period of most
18 intense flux closure in the magnetotail, most often shortly after
19 substorm onset. The ionospheric convection velocity, as measured
20 by SuperDARN, appears to be reduced in the vicinity of the
21 streamer, suggesting de-coupling of magnetospheric and
22 ionospheric plasma flows in the region of enhanced ionospheric
23 conductance.

24 1. Introduction

25 Streamers are auroral features which extend roughly in the north-
26 south direction, that have been unambiguously related to bursty
27 bulk flows (BBF) in the magnetotail [Amm and Kauristie, 2002,
28 and references therein]. They are characterized by enhanced field-
29 aligned currents at their dusk and dawn edges, the current being
30 oriented downward (upward) along the eastern (western)
31 boundary. Several studies have suggested that reconnection plays
32 a role in the dynamics of BBFs [Angelopoulos *et al.*, 1992;
33 Shiokawa *et al.*, 1997; Fairfield *et al.*, 1999, Chen and Wolf,
34 1993].

35 We have developed of a method that combines global remote
36 sensing of the proton aurora with SI12 and measurements of the
37 ionospheric convection with SuperDARN to estimate the location
38 of the open/closed field line boundary, the open flux and the
39 opening and closure rates of magnetic flux [Hubert *et al.*, 2006 *a*].
40 The accuracy of the method was discussed by Hubert *et al.* [2006
41 *a*]. The electric field in the frame of reference of the moving
42 open-closed boundary is computed and integrated along the
43 boundary to retrieve the opening and closure reconnection rates.
44 This method has already been applied to several substorm cycles
45 and to cases of interplanetary shocks [Hubert *et al.*, 2006 *a,b*]. In
46 the present work, we use the method to investigate the relative
47 contribution of auroral streamers in global magnetic flux transfer
48 during a substorm event. The role of BBFs as flux carriers have
49 been estimated e.g. by Angelopoulos *et al.*, (1992) from the basis
50 of magnetospheric in situ observations which provide accurately
51 plasma flow characteristics but lack the global context.

52 2. Observation of a streamer

53 2.1. Data availability.

54 Images of the proton aurora were recorded by the SI12 instrument
55 of the IMAGE satellite [Mende *et al.*, 2000]. The velocity of the

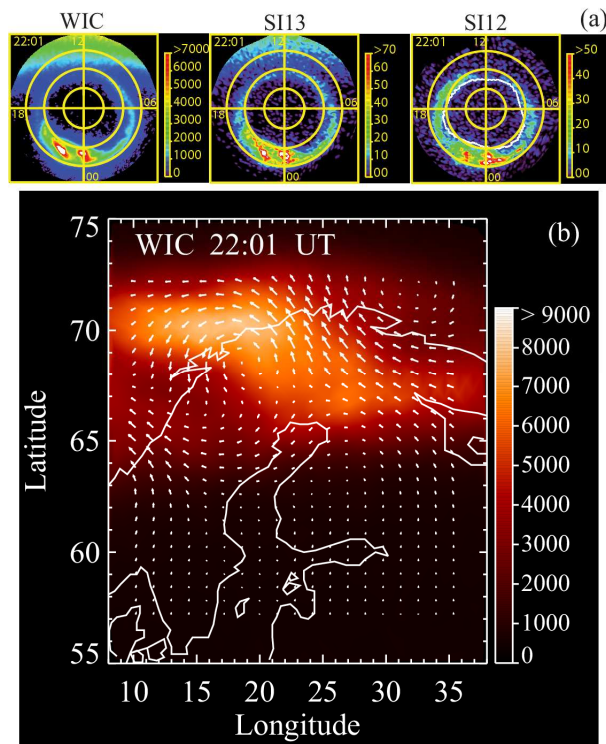
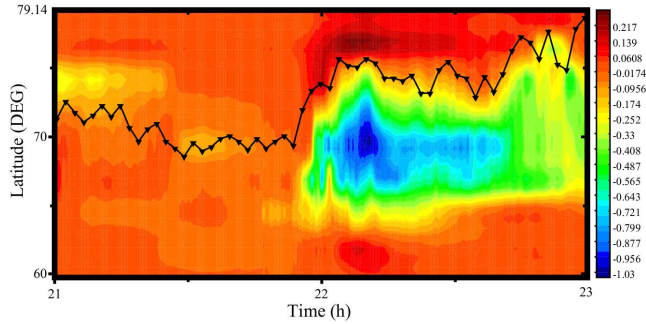


Figure 1. a) Polar view of the IMAGE-FUV WIC, SI13 and SI12 images (magnetic coordinates), with the open/closed field line boundary overlaid on the SI12 image at 2201 UT. b) Map of the ionospheric equivalent currents above Scandinavia (geographic coordinates) in arbitrary units, with the auroral signal from the WIC image in AD units.

1
2
3
4
5
6
7
8
9
10 ionospheric convection is obtained from the Super Dual Auroral
11 Radar Network (SuperDARN) measurements, and the ionospheric
12 electric field is deduced by applying the method developed by
13 *Ruohoniemi and Baker* [1998]. The Wide band Imaging Camera
14 (WIC) and the Spectrographic Imager at 135.6 nm (SI13)
15 instruments of the IMAGE-FUV experiment, which are mostly
16 sensitive to the emissions of the electron aurora, are also used to
17 examine the morphology of the auroral features.
18 On 7 December 2000, the IMAGE-FUV instruments observed a
19 substorm expansion following an onset at 2147 UT. The event
20 started after an interval of southward IMF which had led to the
21 accumulation of open magnetic flux, as evidenced below by the
22 expansion of the auroral oval. The substorm activity was seen as a
23 ~550 nT disturbance in the AE indices. At 2158 UT WIC
24 recorded first signatures of the formation of north-south aligned
25 auroral structures within the auroral bulge. The clearest images of
26 two coincidental auroral streamers were acquired by the WIC and
27 SI13 imagers around 2202 UT (Figure 1a) while by 2206 UT the
28 structures had faded away. One of the streamers was located
29 above northern Scandinavia, which makes it possible to combine
30 space-based data with the ground based observations in that
31 region (midnight). For the other streamer which was located in the
32 ~2200 MLT sector, ground-based data are not available. The
33 open-closed field line boundary determined from the SI12 image
34 at 2201 UT, when the streamers were formed, is presented in
35 Figure 1a. SuperDARN data were available at that time. The data
36 coverage was moderately good. Echoes were recorded above
37 Scandinavia, where the midnight streamer is observed, and above
38 Iceland, not far from the location of the second streamer, thus
39 allowing to constrain the fit used to obtain the ionospheric electric



1
2 Figure 2. East-west equivalent currents (negative values
3 correspond to westward currents, unit A/m) deduced from the
4 MIRACLE - IMAGE magnetometer network, with the SI12
5 open/closed boundary overlaid in black (MLT \approx UT+2.5).
6

7 field in the region of interest.

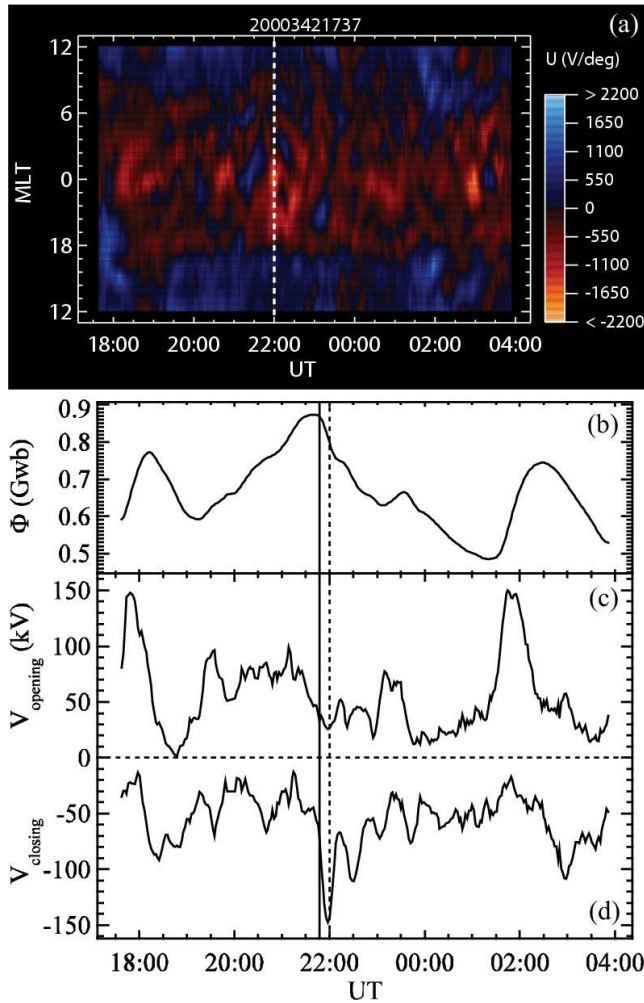
8 2.2. Ionospheric equivalent current, and FUV observations.

9 The ionospheric equivalent current pattern was retrieved using the
10 MIRACLE-IMAGE magnetometer chain operated in Scandinavia
11 (Figure 1b) [Amm and Viljanen, 1999 a]. The streamer develops
12 shortly after 2200 UT following the expansion onset at 2147 UT.
13 A map of equivalent current (EC) obtained at 2201 UT is
14 presented in Figure 1b, with the corresponding part of WIC image
15 overlaid. The EC pattern of figure 1b presents strong poleward
16 currents flowing roughly along the streamer direction and a
17 counterclockwise vortex on the western side of the current
18 channel, consistently with previous studies [Amm et al., 1999 b,
19 Kauristie et al., 2003]. Assuming an homogeneous conductance,
20 this vortex can be associated with upward field aligned currents
21 (FACs). When the streamer developed, the westward equivalent
22 current moved poleward in concert with the poleward motion of
23 the polar cap boundary deduced from the SI12 observations.
24 Figure 2 shows the EC intensity versus latitude and time in the
25 midnight sector as deduced from upward continued
26 magnetometer data [Mersmann et al., 1979] with the polar cap
27 boundary identified from SI12 overplotted in black. This figure
28 suggests a close relationship between the poleward boundary of
29 the electrojet, the poleward optical boundary of the Doppler-
30 shifted Lyman- α emission and the polar cap boundary.

31 2.3. Reconnection at the northern edge of the streamer.

32 The location and motion of the open-closed field line boundary
33 have been retrieved from the SI12 auroral images. The
34 ionospheric electric field deduced from the SuperDARN data is
35 then coupled with these results to estimate the electric field in the
36 reference frame of the moving boundary, and hence the
37 reconnection rates. Figure 3a shows a UT-MLT plot of the
38 differential reconnection voltage along the open-closed boundary
39 $\frac{\delta V}{\delta \text{MLT}}$ (with MLT given in degrees), i.e. the voltage per unit

40 MLT degree, which is proportional to $\vec{E} \cdot d\vec{l}$. Red (blue) shades
41 correspond to negative (positive) voltages, i.e. a closure of open
42 (opening of closed) magnetic flux, respectively. The flux closure
43 rate was clearly intensified in the midnight sector around the time
44 of streamer appearance. Closure rates were high between 1800
45 and 0100 MLT and, in particular along field lines threading the
46 poleward edges of both streamers. A more global view is shown
47 in Figure 3b-d where we present both the open magnetic flux
48 (panel b) and opening and closure voltages (panels c and d)
49 deduced from the IMAGE-FUV and SuperDARN observations.



1
2 Figure 3. Differential reconnection voltage (a), open flux (b),
3 opening voltage (c) and closure voltage (d) obtained from
4 SII2 and SuperDARN observations on 7 December 2000. The
5 solid vertical line indicates the substorm onset, and the dotted
6 vertical lines indicate the development of the auroral streamer.
7

8 Due to reconnection at the dayside magnetopause, the
9 magnetosphere accumulates up to ~ 0.9 GWb of open flux until
10 the onset of the substorm expansion phase. The flux closure
11 voltage then reaches ~ 150 kV around 2200 UT, indicating very
12 intense nightside reconnection at that time.

13 We have also integrated $\vec{E} \cdot d\vec{l}$ along the open/closed boundary in
14 the MLT sector corresponding to the poleward edge of the
15 observed streamer (2255 to 2330 MLT) to determine the
16 associated closure voltage (Figure 4). A strong increase of the
17 reconnection voltage is observed around 2200 UT, reaching a
18 maximum of ~ 25 kV. The oscillations observed in the closure
19 voltage in Figure 3 between 2200 and 2330 UT with a period of
20 roughly 30 min are also found when we restrict our attention to
21 that narrow MLT sector, and are due to changes in the poleward
22 velocity of the boundary. In general, the motion of the boundary
23 produces the main contribution to the closure voltage during the
24 expansion phase, as can be expected from the rapid poleward
25 expansion of the substorm auroral bulge. In the present case, this
26 dominance reduces the impact of potential uncertainties related
27 with the limited SuperDARN data coverage in some areas. We
28 suggest that these oscillations are not specific to the streamer
29 itself, because its lifetime is much shorter than the 30 min period.
30 The MLT sector of the streamer contributes less than 20 % to the

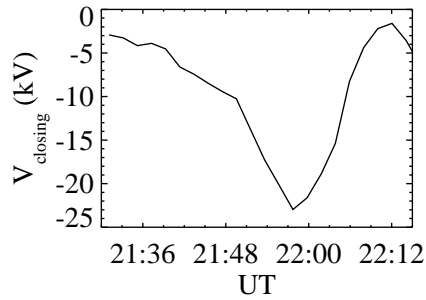


Figure 4. Closure voltage derived from the line integral of the electric field along the open-closed field line boundary in the MLT sector where the auroral streamer is observed.

total, and the oscillations of the closure voltage appear as a global process probably related with the development of the substorm expansion phase. Similar results can be obtained concerning the second streamer located in the premidnight sector. Note that the period of ~ 30 min lies in the range of Pc6 pulsations.

3. Discussion

We discuss observations of a typical streamer which developed during the early stage of a substorm expansion phase, when the flux closure voltage dramatically increased after the onset to reach a maximum magnitude of ~ 150 kV. The time coincidence between the formation of the streamer and strong overall flux closure rate shortly after the onset suggests a possible causal relation between these two phenomena. However, intense flux closure may not be the only condition necessary to form BBFs and auroral streamers. An enhanced flux closure is the natural signature of the substorm expansion phase, and the simultaneous appearance of the streamer may be considered incidental, unless a mechanism linking BBF's and flux closure would exist.

The flux tubes threading a BBF consists of a so called "plasma bubble" flowing fast Earthward in the tail [Sergeev *et al.*, 2004; Chen and Wolf, 1993, 1999]. In the case of BBF's and under the frozen-in approximation, the flux tubes that go through closure must be initially depleted compared to the surrounding medium, as BBF's present a low plasma density. This might be due either to localised time-dependence of the lobe plasma density flowing into the reconnection region, or to a localised displacement (e.g. earthward) of the reconnection region itself. Now the initial earthward-directed velocity of the newly-closed flux tubes and accelerated plasma following tail reconnection is $\sim V_A$, the Alfvén speed in the tail lobes [see e.g. Owen and Cowley, 1987]. Since V_A is larger for lower plasma density with a given tail lobe field strength, it is inevitable that a localised reduction in the lobe plasma density on the newly-closed flux tubes, due e.g. to one or other of the above effects, will produce a localised channel of higher-speed earthward flow in the plasma sheet. From this standpoint, the high velocity of the plasma flowing out of the reconnection site does not stem from the value of the reconnection rate itself, but from the value of the Alfvén velocity characterizing the plasma entering the reconnection region. The observations presented here show that the related reconnection rates also become enhanced, indicating an enhancement in the reconnection-associated cross-tail electric field E_y in the tail. Since the earthward contraction speed of the newly-closed flux tubes is given by $E_y/B_z \approx V_A$, where B_z is the field component threading through the current sheet, the implication is that $B_z \approx E_y/V_A$ would also become enhanced in a region where the increase of E_y would dominate that of V_A . Regions of high-speed low-density plasma threaded by a strong B_z are indeed the defining features of

1 BBFs. Within this scenario, the interchange instability mechanism
2 proposed by *Chen and Wolf* [1993, 1999] might operate in a later
3 phase of flux-tube evolution, once the initial contraction following
4 tail reconnection is over.

5 SuperDARN radar data obtained above Northern Scandinavia
6 between 2200 and 2202 UT reveal that the ionospheric convection
7 was very low within the streamer, below 200 m s^{-1} . This reduced
8 convection suggests that the strong auroral precipitation
9 (responsible for the bright signatures in the IMAGE-FUV images)
10 caused intense ionisation of the atmospheric gas thus favoring
11 ionospheric field line tying [*Coroniti and Kennel*, 1973], which
12 does not exclude strong flows from occurring along the same field
13 line in the equator plane, and allows some decoupling between the
14 magnetospheric and ionospheric plasma flows in mesoscale
15 structures. A highly conductive ionosphere is able to discharge
16 efficiently the electric potentials of magnetospheric origin which
17 can be considered as a cause for the decoupling. In-situ data from
18 the tail (which are not available for the interval discussed here)
19 would be necessary to rigorously establish that the observed
20 streamer was actually related with a BBF.

21 In order to consolidate the relation between flux closure and
22 streamer formation on observational grounds, we analyzed the
23 reconnection voltage of eleven other intervals with a north-south
24 aligned arc, observed with IMAGE-FUV during winter 2000 on
25 10/02, 1109 UT; 10/03, 0339 UT; 10/07 0758 UT; 10/29, 0420
26 UT; 11/01, 0558 UT; 11/03, 2345 UT; 11/29, 0147 UT; 12/08,
27 0258 UT, 12/23, 0802 UT; 12/23, 1023 UT and 12/23, 1207UT.
28 Despite the limited radar data coverage of some of these events,
29 these intervals show a relation between streamers and flux
30 closure. Higher closure voltages appear to favor the appearance of
31 streamers: the closure voltage was found to range between \sim -50
32 and \sim -125 kV in all cases but one (11/03/2000). In this latter case,
33 the voltage was only 22 kV, but the polar edge of the streamer
34 was located in the MLT sector threaded by the field lines along
35 which the flux closure takes place. Cases with higher closure
36 voltages were found during an expansion phase, or shortly after
37 during the recovery phase. Surprisingly, considering longer time
38 scales, most of these streamers were observed during or following
39 an interval of disturbed Dst index (8 cases with $\text{Dst} < -30 \text{ nT}$, and
40 up to $\text{Dst} \sim -127 \text{ nT}$).

41 Observations of dipolarized field lines threading BBFs by
42 *Angelopoulos et al.* [1992] indeed relate BBFs to magnetic flux
43 closure. The time resolution of our method (\sim 15 min) does not
44 however allow us to fully resolve transient reconnection on these
45 time scales, so that we may have missed a transient signature
46 directly associated with the formation of the streamer. The time
47 lag reported by *Angelopoulos et al.* [1992] between the BBF
48 acceleration and the magnetic dipolarization may suggest that the
49 plasma threaded by newly closed field lines evolve slowly uptail
50 from the reconnection site until the conditions necessary for an
51 additional acceleration mechanism are met, due to a specific
52 topology of the electromagnetic field and of the current system.
53 Possible candidates to accelerate the plasma bubble are again the
54 $\vec{j} \times \vec{B}$ force, and the interchange instability proposed by *Chen and*
55 *Wolf* [1993, 1999], for example. Another possibility may be that
56 the onset of reconnection takes place under some conditions that
57 differ from those favoring the formation of BBF's, so that a BBF
58 will not form until other open flux tubes with the suitable
59 properties will have reached the X-line, after the formation of the
60 reconnection site.

61 In this study, the ionospheric equivalent currents deduced from
62 the MIRACLE-IMAGE and the S112 boundary identification

1 consistently indicate that the polar boundary moved poleward
2 prior to the streamer development (Figure 2) indicating that flux
3 closure started before the formation of the streamer. Indeed, the
4 substorm expansion onset appeared in the FUV images ~13 min
5 before the streamer. However, a more extensive study including
6 in-situ measurements in the tail is needed to fully verify the
7 scenario proposed above. Note that the transition between the
8 stretched tail and the dipolarized BBF can be idealized by a field
9 changing orientation along a helix, with a curl parallel to the field
10 implying field-aligned currents compatible with the usual current
11 pattern of an auroral streamer.

12 4. Summary

13 An auroral streamer was observed to develop in the midnight
14 sector during a substorm expansion phase on 7 December 2000
15 between 2200 and 2206 UT using the MIRACLE-IMAGE
16 magnetometer network, the FUV instruments onboard the
17 IMAGE satellite, and the SuperDARN radar network. The open
18 flux accumulated prior to onset was high, reaching ~0.9 GWb.
19 The flux closure voltage, oscillating with a period of ~30 min,
20 reached a maximum magnitude of ~150 kV roughly at the time of
21 the formation of the streamer. The reconnection rate also reached
22 a maximum on field lines threading the poleward edge of the
23 streamer. Ionospheric convection data suggest ionospheric field
24 line tying and consequent decoupling of magnetospheric and
25 ionospheric flows in the vicinity of the streamer. The closure
26 voltage computed here is consistent with a BBF formed by the
27 closure of plasma-depleted open flux tubes some time after the
28 reconnection onset, with high plasma velocity at the exit of the
29 reconnection site due to the $\vec{j} \times \vec{B}$ acceleration and possibly
30 followed by the set up of an interchange instability. The relation
31 linking flux closure and north-south aligned arcs is also found for
32 eleven other cases observed with IMAGE-FUV.

33 Acknowledgements. B. Hubert is supported by the Belgian National
34 Fund for Scientific Research (FNRS). This work was funded by the
35 PRODEX program managed by ESA in collaboration with the
36 Belgian Federal Science Policy Office. Work at Leicester was
37 supported by PPARC grant PPA/G/O/2003/00013. S.W.H. Cowley
38 was supported by a Royal Society Leverhulme Trust Senior
39 Fellowship. Work at FMI was supported by the Academy of Finland.
40 The MIRACLE and magnetometer (IMAGE) networks are operated
41 as a European collaboration under the leadership of the Finnish
42 Meteorological Institute.

43 References

- 44 Amm O., and A. Viljanen (1999 a), Ionospheric disturbance magnetic
45 field continuation from the ground to the ionosphere using
46 spherical elementary current systems, *Earth Planet. Space*, 51,
47 431.
- 48 Amm O., A. Pajunpää, and U. Brandström (1999 b), Spatial
49 distribution of conductances and currents associated with north-
50 south auroral form during a multiple-substorm period, *Ann.*
51 *Geophys.*, 17, 1385.
- 52 Amm, O. and K. Kauristie (2002), Ionospheric signatures of bursty
53 bulk flows, *Surv. Geophys.*, 23, 1.
- 54 Angelopoulos, V., W. Baumjohann, C.F. Kennel, F.V. Coroniti, M.G.
55 Kivelson, R. Pellat, R.J. Walker, H. Lühr, and G. Paschmann
56 (1992), Bursty bulk flows in the inner central plasmasheet, *J.*
57 *Geophys. Res.*, 97, 4027.
- 58 Chen, C. X., and R.A. Wolf (1993), Interpretation of high-speed flows
59 in the plasma sheet, *J. Geophys. Res.*, 98, 21409.
- 60 Chen, C. X., and R. A. Wolf (1999), Theory of thin-filament motion
61 in Earth's magnetotail and its application to bursty bulk flows, *J.*
62 *Geophys. Res.*, 104, 14613.

1 Coroniti, F. V., and C. F. Kennel (1973), Can the ionosphere regulate
2 magnetospheric convection?, *J. Geophys. Res.*, 78, 2837.
3 Fairfield, D.H., T. Mukai, M. Brittnacher, G.D. Reeves, S. Kokubun,
4 G.K. Parks, T. Nagai, H. Matsumoto, K. Hashimoto, D.A. Gurnett,
5 and T. Yamamoto (1999), Earthward flow bursts in the inner
6 magnetotail and their relation to auroral brightening, AKR
7 intensifications, geosynchronous particle injections and magnetic
8 activity, *J. Geophys. Res.*, 104, 355.
9 Hubert, B. , S.E. Milan , A. Grocott, S. W. H. Cowley, and J.-C.
10 Gérard (2006 a), Dayside and nightside reconnection rates inferred
11 from IMAGE-FUV and SuperDARN data, *J. Geophys. Res.*, 111,
12 A03217, doi:10.1029/2005JA011140.
13 Hubert, B., M. Palmroth, T.V. Laitinen, P. Janhunen, S.E. Milan, A.
14 Grocott, S.W.H. Cowley, T. Pulkkinen, and J.-C. Gérard (2006 b),
15 Compression of the Earth's magnetotail by interplanetary shocks
16 directly drives transient magnetic flux closure, *Geophys. Res. Lett.*,
17 33, L10105, doi:10.1029/2006GL026008
18 Kauristie, K., V.A. Sergeev, O. Amm, M.V. Kubyshkina, J. Jussila, E.
19 Donovan, and K. Liou (2003), Bursty bulk flow intrusion to the
20 inner plasma sheet as inferred from auroral observations, *J.*
21 *Geophys. Res.*, 108, 1040, doi: 10.1029/2002JA009371.
22 Mende, S.B., H. Heeterks, H.U. Frey, J.M. Stock, M. Lampton, S.
23 Geller, R. Abiad, O. Siegmund, S. Habraken, E. Renotte, C. Jamar,
24 P. Rochus, J.C. Gérard, R. Sigler, and H. Lauche (2000), Far
25 ultraviolet imaging from the IMAGE spacecraft : 3. Spectral
26 imaging of Lyman alpha and OI 135.6 nm, *Space Sci. Rev.*, 91,
27 287.
28 Mersmann, U., W. Baumjohann, F. Küppers, and K. Lange (1979),
29 Analysis of an eastward electrojet by means of upward
30 continuation of ground-based magnetometer data, *J. Geophys.*, 45,
31 281-298.
32 Owen, C. J., and S. W. H. Cowley (1987), Simple models of time-
33 dependent reconnection in a collision-free plasma with an
34 application to substorms in the geomagnetic tail, *Planet. Space*
35 *Sci.*, 35, 451.
36 Ruohoniemi, J. M., and K.B. Baker (1998), Large scale imaging of
37 high latitude convection with Super Dual Auroral Radar Network
38 HF radar observations, *J. Geophys. Res.*, 103, 20797.
39 Sergeev V.A., K. Liou, P.T. Newell, S.-I. Otani, M.R. Hairson, and F.
40 Rich (2004), Auroral streamers: characteristics of associated
41 precipitation, convection and field-aligned currents, *Ann.*
42 *Geophys.*, 22, 537.
43 Shiokawa, K., W. Baumjohann, and G. Haerendel (1997), Braking of
44 high-speed flows in the near-Earth tail, *Geophys. Res. Lett.*, 24,
45 1179.
46
47